Journal of Zhejiang University-SCIENCE C (Computers & Electronics)
ISSN 1869-1951 (Print); ISSN 1869-196X (Online)
www.zju.edu.cn/jzus; www.springerlink.com
E-mail: jzus@zju.edu.cn

Modeling and multiobjective optimization of traction performance for autonomous wheeled mobile robot in rough terrain*

Ozoemena Anthony ANI, He XU†‡, Yi-ping SHEN, Shao-gang LIU, Kai XUE

(*College of Mechanical and Electrical Engineering, Harbin Engineering University, Harbin 150001, China*)

†E-mail: railway_dragon@163.com

Received Aug. 6, 2012; Revision accepted Dec. 7, 2012; Crosschecked Dec. 13, 2012

Abstract: Application of terrain-vehicle mechanics for determination and prediction of mobility performance of autonomous wheeled mobile robot (AWMR) in rough terrain is a new research area currently receiving much attention for both terrestrial and planetary missions due to its significant role in design, evaluation, optimization, and motion control of AWMRs. In this paper, decoupled closed form terramechanics considering important wheel-terrain parameters is applied to model and predict traction. Numerical analysis of traction performance in terms of drawbar pull, tractive efficiency, and driving torque is carried out for wheels of different radii, widths, and lug heights, under different wheel slips. Effects of normal forces on wheels are analyzed. Results presented in figures are discussed and used to draw some conclusions. Furthermore, a multiobjective optimization (MOO) method for achieving optimal mobility is presented. The MOO problem is formulated based on five independent variables including wheel radius r, width b, lug height h, wheel slip s, and wheel rotation angle θ with three objectives to maximize drawbar pull and tractive efficiency while minimizing the dynamic traction ratio. Genetic algorithm in MATLAB is used to obtain optimized wheel design and traction control parameters such as drawbar pull, tractive efficiency, and dynamic traction ratio required for good mobility performance. Comparison of MOO results with experimental results shows a good agreement. A method to apply the MOO results for online traction and mobility prediction and control is discussed.

Key words: Autonomous wheeled mobile robot (AWMR), Terramechanics, Traction, Motion control, Multiobjective optimization (MOO), Genetic algorithm (GA)

doi:10.1631/jzus.C12a0200 **Document code:** A **CLC number:** TP24

1 Introduction

Vehicle traction mechanics is concerned with the interaction between the mobility devices usually called running gears, such as the wheel, track, leg, air cushion, and various types and conditions of terrains over which the vehicles traverse. There is an increasing need for studies on the terrain properties in relation to vehicle characteristics to have an adequate understanding of a vehicle's mobility performance for the major purposes of effective design and motion control. Young *et al*. (1984) stated that the problem of determination and prediction of the capability of a particular piece of vehicle to successfully traverse over a specific terrain is just recently receiving good attention. Schenker *et al*. (2003) noted that the subject of terramechanics appears to be a fairly new research focus in rover design. Iagnemma and Dubowsky (2004) stated that wheel-terrain interaction plays a critical role in rough-terrain mobility; for example, the knowledge of terrain information is a major consideration in traction control problems. According to Wong (2010), systematic studies of the principles underlying the rational development of off-road

‡ Corresponding author

* Project supported by the National Natural Science Foundation of China (No. 60775060), the Natural Science Foundation of Heilongjiang Province of China (No. F200801), the Specialized Research Fund for the Doctoral Program of Higher Education (Nos. 200802171053 and 20102304110006), and the Harbin Science and Technology Innovation Talents Special Fund (No. 2012RFXXG059), China

vehicles did not receive significant attention until the middle of the 20th century. He further stated that the works of Bekker (1956; 1960; 1969) were foundation works and the initial stimulator that triggered the interest of many researchers in this direction. Ding *et al*. (2011b) reported that terramechanics is becoming a new research hotspot, as it plays an important role in meeting the increasing new challenges facing planetary exploration missions. They further noted that optimizing the control strategies of wheeled mobile robots (WMRs) on the basis of terramechanics is important for locomotion, path following, and path planning, especially on rough and deformable terrain.

Konjicija and Avdagić (2009) used a multiobjective genetic algorithm (GA) to solve a problem about synthesis of control of a mobile robot in an unknown environment. In trying to obtain an optimal configuration of an autonomous WMR (AWMR) for mobility with respect to orientation and stability, Freitas *et al*. (2010) applied the multiobjective optimization (MOO) method to find the optimal solution for two conflicting objectives. In a simulation platform, Sato and Ishii (2010) used the GA to simultaneously optimize the robot structure and control system to achieve stable travel on continuously uneven surfaces. In the study of the effect of individual parameters on the collective performance of swarm robotic systems, Liu and Winfield (2010) applied a GA to optimize the controller design to achieve optimal behaviors of individual robots engaged in adaptive collective foraging for energy.

General research problems around this area have included: analysis and modeling of wheel-terrain interaction, strategies and methods for slip detection, estimation and compensation, real-time terrain parameter estimation, traction optimization, effective traction control strategies, and algorithm development. Therefore, based on motion control type and techniques, research problems on vehicles can be classified into two broad categories: human controlled and intelligent/autonomous vehicles. Research problems can be further divided into design and development, modeling, motion planning, and motion control (Fig. 1). In this study, we present a precise concept of vehicle traction and mobility on rough and deformable terrain and its modeling using the classical and decoupled closed form terramechanics. This study also tries to obtain the optimal wheel-terrain parameter values required to achieve optimum design of wheels as well as optimum traction and motion control by formulating an MOO problem and solving it in MATLAB using GA.

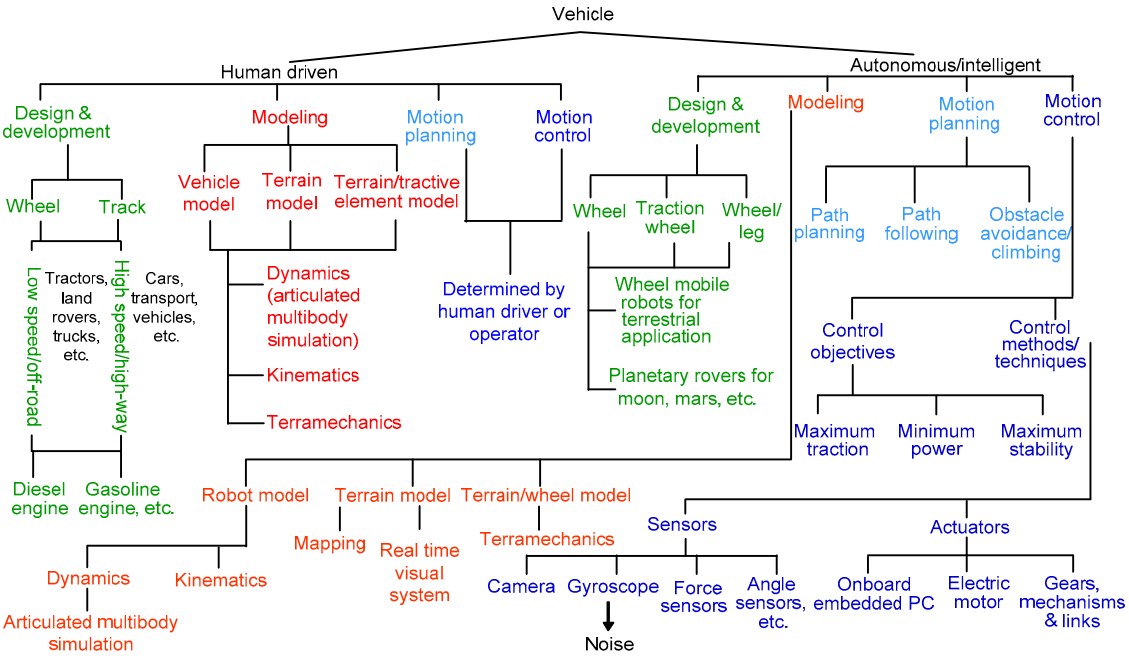

Fig. 1 Schematic of research directions for vehicles based on their motion control type and technique

2 Wheel slippage and traction modeling

2.1 Terramechanics modeling and slippage

Towards meeting the challenge of developing effective navigation and motion control algorithms for AWMR in rough terrain, Iagnemma *et al*. (2001) stated that advanced control and planning methods must be developed that consider the physical characteristics of the rover and its environment including kinematic/force analysis, terrain geometry estimation, and wheel-terrain interaction. Three classes of parameters are important to adequately describe and model wheel-terrain interaction (Fig. 2). These parameters include vehicle/wheel parameters, terrain/soil parameters, and interface/motion parameters (Table 1). A good traction model should connect key components of these three major classes of parameters.

Fig. 3 shows the picture of the WMR (Xu *et al*., 2011) used in this study.

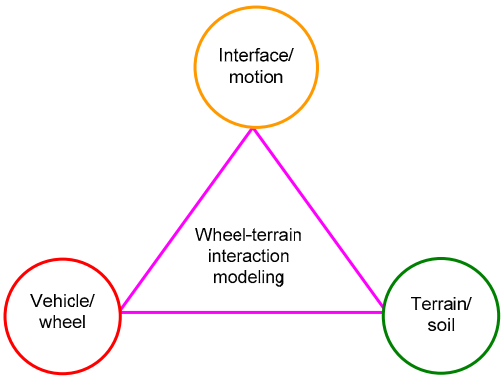

Fig. 2 Traction (wheel-terrain interaction) modeling

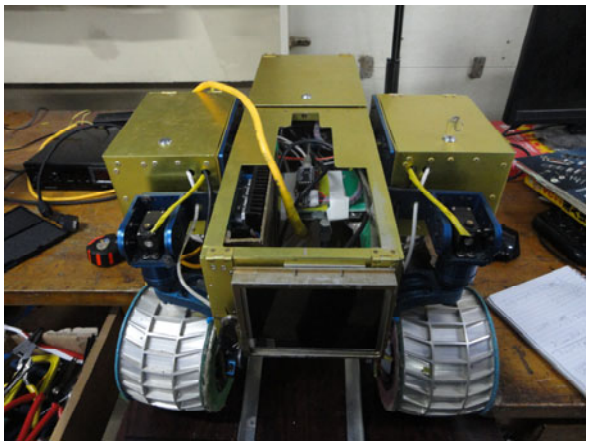

Fig. 3 Picture of wheeled mobile robot (WMR) of Harbin Engineering University (Xu *et al.*, 2011)

Table 1 Description of parameters involved in wheel-soil interaction mechanics

Parameter	Description
Vehicle/wheel parameters	
r (m)	Wheel radius
r_s (m)	Equivalent shearing radius of the wheel
R_j (m)	Effective wheel radius for calculating θ_1'
λ_s	Coefficient used for calculating r_s
b (m)	Wheel width
n_L	Number of wheel lugs
h (m)	Height of lugs
N	Space angle between lugs (°), N=360/n_L
β_L (°)	Inclination angle of wheel lugs
W (N)	Vertical wheel load
T (N·m)	Driving torque generated by the wheel motor and reduction gears
θ (°)	Wheel rotation angle
Terrain/soil parameters	
c (Pa)	Cohesion of soil
φ or ϕ (°)	Internal friction angle of soil
kc (Pa/m^{n+1})	Cohesive modulus of soil
$k\varphi$ (Pa/m^n)	Frictional modulus of soil
n	Constant sinkage exponent of soil
τ_m	Maximum shear stress
τ	Shear stress
σ	Normal stress
k (m)	Shear deformation modulus of soil
Interface/motion parameters	
s	Wheel slip (ratio)
s_{j1}, s_{j2}	Transitional slip ratios
θ_1 (°)	Entrance angle
θ_2 (°)	Exit angle
θ_m (°)	Angle of the maximum stress
θ_1' (°)	Angle where the soil begins to deform
z (m)	Wheel sinkage
v (m/s)	Wheel linear velocity
ω (rad/s)	Wheel angular velocity
c_1, c_2, c_3	Coefficients of wheel-soil interaction angle (used for calculating θ_m)
F_N (N)	Normal force exerted on the wheel by soil
F_{DP} or DP (N)	Drawbar pull exerted on the wheel by soil
M_R (N·m)	Resistance moment exerted on the wheel by soil
PC	Drawbar pull coefficient
TC	Tractive force coefficient
PE	Drawbar pull efficiency
TE	Tractive efficiency
Ks	Lumped pressure-sinkage coefficient

Fig. 4 is a model of a rigid wheel on deformable terrain. The soil will fail, leading to slippage immobilization and sinkage when the shear stress exerted on the terrain by the wheel of the robot exceeds the maximum shear stress of the soil. The maximum shear stress τ_m is given by the Mohr-Coulomb soil failure criterion:

$$\tau_m = c + \sigma_{(m)} \tan\phi. \quad (1)$$

The work of Bekker (1956; 1960) is one of the earliest works on slip and traction modeling that gives the fundamental idea that most researchers (Janosi and Hanamoto, 1961; Gustafsson, 1997; Iagnemma *et al*., 2002; Lindgren *et al*., 2002; Yoshida and Hamano, 2002; Yoshida, 2003; Ojeda and Borenstein, 2004; Reina, 2006; Iagnemma and Ward, 2009) in this field derive from. Bekker (1956; 1960) showed the relationship between shear force and slip for different soils, and gave the model for soil shear/deformation using curves having the form of an over-damped sinusoid. However, Janosi and Hanamoto (1961) proposed a simpler model that can apply to most common soils; they suggested that the shear stress τ and deformation j may be related as follows:

$$\tau = \tau_m (1 - e^{-j/k}), \quad (2)$$

given that k depends on soil properties and that τ_m is obtained from the Mohr-Coulomb soil failure criterion (Eq. (1)).

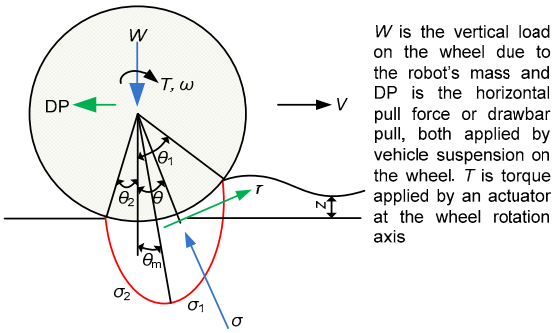

Fig. 4 Model of a rigid wheel on deformable terrain

2.2 Traction performance metrics and modeling in rough terrain

Traction can be defined as the ability of the vehicle's wheel to generate enough force to overcome all types of vehicle-resisting forces and hence keep the vehicle in constant travel (Young *et al*., 1984). Generally, the performance characteristics of off-road vehicles are evaluated based on their functional requirements; however, mobility is a performance metric that cuts across all types of off-road vehicles irrespective of their specific functional requirements. Mobility has to do with the performance of the vehicle in relation to soft terrain, obstacle negotiation and avoidance, ride quality over rough terrain, and water crossing. The vehicle's performance on rough and deformable terrain constitutes a very important problem in vehicle mobility research. Therefore, there is a serious need for a detailed analysis of the relationship among vehicle performances, design parameters, and the terrain (Wong, 2001). Apart from aerodynamic and gravitational forces, all the other major forces and moments that influence vehicle motion are applied through the wheel-terrain contact or contact of other types of running gears. Therefore, a good knowledge of the characteristics of the interaction at the interface between the wheel and the terrain is essential to the study of vehicle performance characteristics. A vehicle wheel should generally support the weight of the vehicle, cushion the vehicle over surface irregularities, provide sufficient traction for driving and braking, as well as provide steering control and stability in the direction of travel.

Many researchers have remarked that traction performance metrics for off-road vehicles in rough and deformable terrain should include all or some of the following parameters: driving torque, ability to accelerate, develop drawbar pull, overcome obstacles, and decelerate. Others include travel reduction (usually called slip), dynamic traction ratio, tractive efficiency, gross traction ratio, net traction ratio (sometimes called pull/weight ratio), motion resistance, and rolling resistance (Goering, 1989; Wong, 2001; Zoz and Grisso, 2003; Schreiber and Kutzbach, 2008; Ding *et al*., 2011a). The drawbar pull is influenced by the performance of the power source as well as traction conditions such as soil and wheel parameters. These traction conditions should be described by a limited number of parameters that can easily be determined. Traction models have been continuously improved over and over again by many researchers to meet the increasing challenges of rover mobility on rough and deformable terrains, especially for planetary exploration and related missions.

Generally, most terrestrial terrains that may be sandy, clayey, and loamy or their combinations exhibit the characteristics of an ideal elastoplastic material. The idea about modeling and analyzing stress distribution in such semi-infinite, homogeneous, isotropic, elastic medium when subjected to a vertical point load applied on the surface was first developed by Boussinesq (Sohne, 1958). Given that $R=\sqrt{z^2+r^2}$, Boussinesq's results gave an expression for the vertical stress σ_z at a point in the elastic medium, thus

$$\sigma_z=\frac{3W}{2\pi R^2}\left(\frac{z}{R}\right)^3=\frac{3W}{2\pi R^2}\cos^3\theta. \tag{3}$$

Since stresses do not depend on the modulus of elasticity of the material, they are functions only of the load applied and the distance from the point of application of the load. Eq. (3) is valid only for calculating stresses at points that are not very close to the point of application of the load. Based on this principle of stress distribution under point loading, the distribution of stresses in an elastic medium subjected to various loading conditions could be predicted by the principle of superposition. For a circular contact area A with radius r_0 and uniform pressure p_0, the vertical stress at depth z below the center of the contact area could be determined given that the load acting upon the contact area is represented by a number of discrete point loads, thus (Bekker, 1956)

$$\mathrm{d}W=p_0\mathrm{d}A=p_0r\mathrm{d}r\mathrm{d}\theta. \tag{4}$$

So from Eq. (3), we have

$$\mathrm{d}\sigma_z=\frac{3}{2\pi}\frac{p_0r\mathrm{d}r\mathrm{d}\theta}{\left(1+(r/z)^2\right)^{\frac{5}{2}}z^2}. \tag{5}$$

The resultant vertical stress σ_z at a depth of z below the center of the contact area is then equal to the sum of the stresses produced by point loads of $p_0r\mathrm{d}r\mathrm{d}\theta$ and could be calculated as follows, given that $u^2=(r/z)^2$:

$$\sigma_z=3p_0\int_0^{r_0/z}\frac{u\mathrm{d}u}{(1+u^2)^{\frac{5}{2}}}=p_0\left(1-\frac{z^3}{(z^2+r_0^{\,2})^{3/2}}\right). \tag{6}$$

For a rigid wheel on a deformable terrain, evaluating the relationship between the tractive effort and the slip requires that the development of shear displacement along the wheel-soil interface be determined first. The shear displacement developed along the contact area of a rigid wheel may be determined based on the analysis of the slip velocity V_j. The slip velocity V_j of a point on the rim relative to the terrain is the tangential component of the absolute velocity at the same point. The magnitude of the slip velocity V_j of a point on the rim defined by angle θ can be expressed by (Wong and Reece, 1967a; 1967b)

$$V_j=r\omega\left(1-(1-s)\cos\theta\right). \tag{7}$$

The slip velocity varies with angle θ and slip for a rigid wheel, so the shear displacement j along the wheel-soil interface is given as

$$\begin{aligned}j&=\int_0^t V_t\,\mathrm{d}t=\int_\theta^{\theta_0}r\omega\left(1-(1-s)\cos\theta\right)\frac{\mathrm{d}\theta}{\omega}\\&=r\left((\theta_0-\theta)-(1-s)(\sin\theta_0-\sin\theta)\right),\end{aligned} \tag{8}$$

where θ_0 is the entry angle that defines the angle where a point on the rim comes into contact with the terrain. The shear stress distribution along the contact patch of a rigid wheel may be determined on the basis of the relationship between the shear stress and shear displacement. Applying the Janosi and Hanamoto (1961) model in Eq. (2), the shear stress distribution could be expressed as a function of the angular location on the wheel rim, thus

$$\begin{cases}\tau=\tau_{\mathrm{m}}(1-\mathrm{e}^{-j/K})=(c+\sigma\tan\phi)(1-\mathrm{e}^{-j/K}),\\ \tau(\theta)=\left(c+\sigma(\theta)\tan\phi\right)(1-\mathrm{e}^{-j/K})=\left(c+\sigma(\theta)\tan\phi\right)\\ \cdot\left(1-\exp\left(-(r/K)\left(\theta_0-\theta-(1-s)(\sin\theta_0-\sin\theta)\right)\right)\right).\end{cases} \tag{9}$$

The total tractive effort F can be determined by integrating the horizontal component of the tangential stress over the entire contact patch area, thus

$$F=\int_0^{\theta_0}\tau(\theta)\cos\theta\mathrm{d}\theta. \tag{10}$$

The vertical component of shear stress at the contact area supports part of the vertical load on the wheel; therefore, the complete equations for predicting the tractive performance of a rigid wheel on deformable terrain could be expressed as follows.

For vertical load W,

$$W = rb\left(\int_0^{\theta_0} \sigma(\theta)\cos\theta \mathrm{d}\theta + \int_0^{\theta_0} \tau(\theta)\sin\theta \mathrm{d}\theta\right). \quad (11)$$

For drawbar pull F_d,

$$F_\mathrm{d} = rb\left(\int_0^{\theta_0} \tau(\theta)\cos\theta \mathrm{d}\theta - \int_0^{\theta_0} \sigma(\theta)\sin\theta \mathrm{d}\theta\right), \quad (12)$$

and for torque T,

$$T_\mathrm{w} = r^2 b\int_0^{\theta_0} \tau(\theta)\mathrm{d}\theta. \quad (13)$$

Herein z is the wheel sinkage, n is the sinkage exponent, k_1 and k_2 are the pressure sinkage moduli, b is the width of the wheel, j is the shear deformation distance, ϕ is the angle of internal friction, k is the shear deformation modulus, and c is the cohesion of soil. The distribution of normal stress (Eq. (3)) could be expressed as a function of the angular location on the wheel rim denoted as θ, in line with a relationship that exists between the radius of the wheel r, z, and θ. Thus (Shibly *et al*., 2005),

$$\sigma_1(\theta) = (k_1 + k_2 b)(r/b)^n(\cos\theta - \cos\theta_1)^n, \quad (14)$$

$$\sigma_2(\theta) = (k_1 + k_2 b)(r/b)^n \cdot\left(\cos\left(\theta_1 - \frac{\theta(\theta_1 - \theta_\mathrm{m})}{\theta_\mathrm{m}}\right) - \cos\theta_1\right)^n, \quad (15)$$

where θ_m is the angular location of the maximum normal stress.

In Fig. 4, stress distribution is represented in two parts as σ_1 and σ_2. The normal stress around the wheel rim starts from zero at the free surfaces, and increases to the maximum at θ_m, which is expressed as (Wong and Reece, 1967a; 1967b)

$$\theta_\mathrm{m} = (c_1 + c_2 s)\theta_1, \quad (16)$$

where c_1 and c_2 are constant coefficients.

The normal stress and shear stresses at the front and rear parts of the contact patch area are further simplified as follows (Shibly *et al*., 2005):

$$\sigma_1(\theta) = \frac{\theta_1 - \theta}{\theta_1 - \theta_\mathrm{m}}\sigma_\mathrm{m}, \quad (17)$$

$$\sigma_2(\theta) = \frac{\theta}{\theta_\mathrm{m}}\sigma_\mathrm{m}, \quad (18)$$

$$\tau_1(\theta) = \frac{\theta_1 - \theta}{\theta_1 - \theta_\mathrm{m}}\tau_\mathrm{m}, \quad (19)$$

$$\tau_2(\theta) = \frac{\theta}{\theta_\mathrm{m}}\tau_\mathrm{m}. \quad (20)$$

So for the system shown in Fig. 4, the force balance equations can be determined by integrating the shear and normal stress equations over the contact areas. In real life situations, since θ_2 is usually small and negligible for low cohesion soils, it is assumed that θ_2=0. The traction performance metrics such as the drawbar pull DP, vertical load W, driving torque T, dynamic traction ratio DTR, and the tractive efficiency TE could all be determined. However, note that these traction prediction equations have certain shortfalls when considered for application in developing effective motion control algorithms to meet the increasingly challenging situations usually encountered in both planetary and terrestrial explorations of AWMRs. For instance, in motion control algorithms, the error introduced by cumulative approximations in the integration formula cannot be neglected. Moreover, certain new variables of the wheel, soil, and interface that were not considered in previous traction models or rovers are also important and have been researched recently. Some of the new variables considered in terramechanics include wheel lug height h, lug number n_L, shearing radius r_s (i.e., average radius where the shearing between moving soil and static soil occurs), and lug shearing coefficient λ_s, which fully models the influence of lugged wheels. Ding *et al*. (2009; 2011a) presented decoupled closed form equations for the vertical load, driving torque, drawbar pull, and tractive efficiency, respectively, which have attempted to address some of the shortfalls mentioned, as follows:

$$W = rbA\sigma_\mathrm{m} + \frac{BT}{r_\mathrm{s}c}, \quad (21)$$

$$T=\frac{r_s^2CD\left(bc+\dfrac{W\tan\psi}{rA}\right)}{1+\dfrac{r_sBD\tan\psi}{rA}}, \tag{22}$$

$$\mathrm{DP}=\left(\frac{A^2+B^2}{r_s\,AC}\right)T-\left(\frac{B}{A}\right)W. \tag{23}$$

The following parameters are modeled using the newly considered variables of wheel, soil, and interface as defined in Table 1:

$$r_s=r+\lambda_s h, \tag{24}$$

$$\theta_2=c_3\theta_1, \tag{25}$$

$$\theta_1=a\cos[(r-z)/r], \tag{26}$$

$$\sigma_m=K_s r^N(\cos\theta_m-\cos\theta_1)^N, \tag{27}$$

$$R_j=\begin{cases} r+h, & 0\le s\le S_{j1},\\ r+\dfrac{h(S_{j2}-s)}{S_{j2}-S_{j1}}, & S_{j1}<s<S_{j2},\\ r, & S_{j2}\le s\le 1, \end{cases} \tag{28}$$

$$\theta_1'=a\cos\left(\frac{r-z}{R_j}\right), \tag{29}$$

$$\tau_m=(c+\sigma_m\tan\phi)\cdot\left(1-\exp\left(-r_s\frac{(\theta_1'-\theta_m)-(1-s)(\sin\theta_1'-\sin\theta_m)}{k}\right)\right), \tag{30}$$

$$A=\frac{\cos\theta_m-\cos\theta_2}{\theta_m-\theta_2}+\frac{\cos\theta_m-\cos\theta_1}{\theta_1-\theta_m}, \tag{31}$$

$$B=\frac{\sin\theta_m-\sin\theta_2}{\theta_m-\theta_2}+\frac{\sin\theta_m-\sin\theta_1}{\theta_1-\theta_m}, \tag{32}$$

$$C=\frac{\theta_1-\theta_2}{2}, \tag{33}$$

$$D=1-\exp\left(-r_s\frac{(\theta_1'-\theta_m)-(1-s)(\sin\theta_1'-\sin\theta_m)}{k}\right). \tag{34}$$

Then the dynamic traction ratio and the tractive efficiency can be calculated as

$$\mathrm{DTR}=\mathrm{DP}/W, \tag{35}$$

$$\mathrm{TE}=\frac{\mathrm{DP}\cdot r_s(1-s)}{T}. \tag{36}$$

3 Results of numerical analysis of traction performance

3.1 Tractive efficiency with respect to wheel slip and radius

Generally, the WMR parameters considered in the numerical simulation are based on the existing design parameters of a 5-WMR in our laboratory as well as other designs found in the literature. Similarly, the terrain parameters considered are based on the characteristics of the selected soil/terrain type used in our test bed and available related information in the literature. The results of numerical simulation of traction performance in terms of tractive efficiency for five wheels of different radii 0.075, 0.0885, 0.135, 0.157 35, and 0.20 m for different wheel slips ranging from 0.0 to 1.0 are presented in Fig. 5.

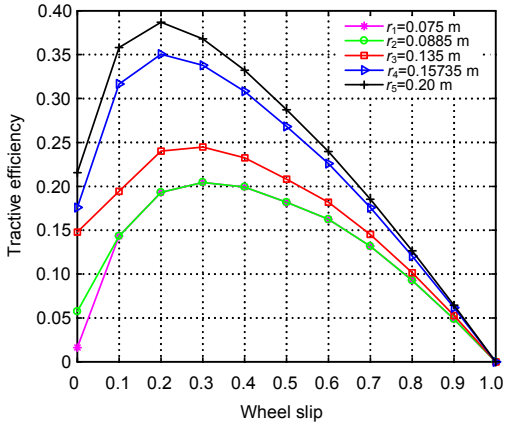

Fig. 5 Tractive efficiency vs. wheel slip for different wheel radii

The wheel width is fixed. Results show that for the different wheel radii considered, tractive efficiency initially increased with increasing slip until a maximum after which it decreases with increasing slip. It is observed that the first three wheels of smaller radii reached their maximum tractive efficiency at a slip of about 0.3, while the last two wheels of larger radii reached their maximum tractive efficiency at a slip of about 0.2. Generally for the same soil condition, wheels of larger radii had higher tractive efficiency.

3.2 Tractive efficiency with respect to wheel slip and width

The results of numerical simulation of traction performance in terms of the tractive efficiency for

seven wheels of different widths 0.10, 0.110, 0.1138, 0.115, 0.120, 0.130, and 0.165 m and under the wheel slip ranging from 0.0 to 1.0 are presented in Fig. 6.

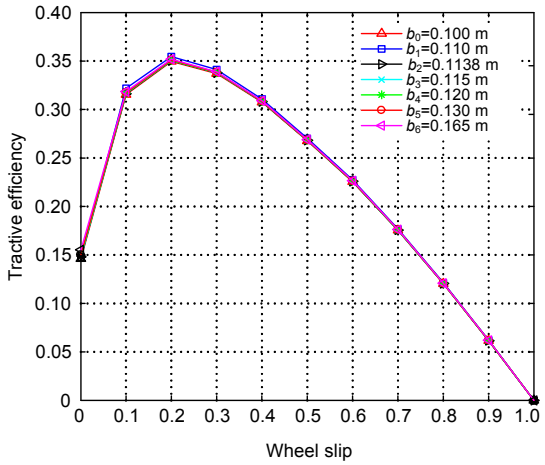

Fig. 6 Tractive efficiency vs. wheel slip for different wheel widths

The wheel radii are fixed to one value. Results show that for the same soil condition and wheel radius, the effect of wheel width on the tractive efficiency is negligible. This implies that the wheel width is not a crucial factor in design when considering tractive efficiency alone; however, it will be an important factor when considering other factors having direct and significant relationship with it, for example, when considering the wheel contact area at the wheel-ground interface that affects the drawbar pull.

3.3 Tractive efficiency with respect to wheel slip and lug height

The results of numerical simulation of traction performance in terms of tractive efficiency for six different wheel lug heights 0.00776, 0.01, 0.015, 0.02, 0.025, and 0.03 m and under the wheel slip ranging from 0.0 to 1.0 are presented in Fig. 7. The width and radii are fixed. For the same soil condition, the maximum tractive efficiency is 0.35 for the smallest lug height 0.00776 m, and 0.45 for the largest lug height of 0.03 m, which both occurred at a wheel slip of 0.2. This indicates that the tractive efficiency generally increases as lug height increases until a certain optimum wheel slip where it begins to decrease afterwards. This implies that lug or grouser height is an important design parameter for WMR moving on rough terrain.

3.4 Drawbar pull with respect to wheel slip and weight of WMR

The results of numerical simulation of traction performance in terms of drawbar pull for four different normal loads of 35, 36.75, 80, and 150 N and under the wheel slip ranging from 0.0 to 1.0 are presented in Fig. 8. For the same soil condition, results show that the drawbar pull increases with the slip. A normal load of 150 N exerted on the wheel due to the weight of the WMR, at a wheel slip of 0.2 requires a pull force of about 32 N to produce forward thrust in the direction of the force while 35 and 36.75 N normal loads at the same wheel slip of 0.2 require about 8 N drawbar pull force. It is observed that the total weight of the rover is an important design parameter when considering the traction performance of WMR in rough terrain. Therefore, it is necessary to determine the optimum weight with respect to other parameters.

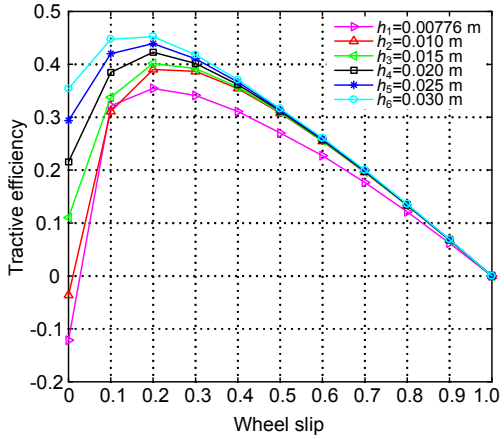

Fig. 7 Tractive efficiency vs. wheel slip for different lug heights

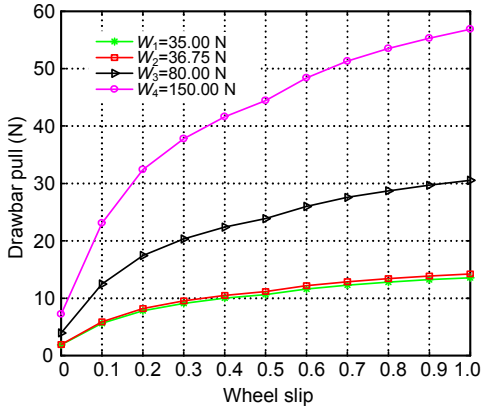

Fig. 8 Drawbar pull vs. wheel slip for different normal loads

3.5 Driving torque with respect to wheel slip and weight of WMR

The results of numerical simulation of traction performance in terms of driving torque for four different normal loads of 35, 36.75, 80 and 150 N and under the wheel slip ranging from 0.0 to 1.0 are presented in Fig. 9. Results show that the driving torque increases as the wheel slip increases. For the same soil condition and at a wheel slip of 0.2, a normal load of 150 N required a driving torque of about 5.5 N·m, while 35 and 36.75 N loads required about 1.4 N·m. Higher driving torque will mean higher power requirement to turn the wheels and hence the selection of the electric motor to power the WMR. Generally one goal of design optimization is to gain higher mechanical advantage, so this information is very useful.

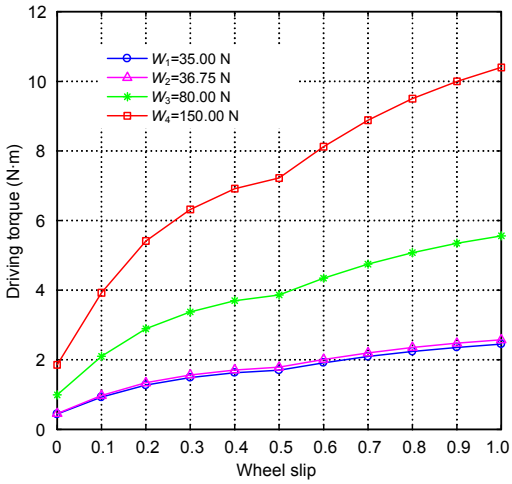

Fig. 9 Driving torque vs. wheel slip for different normal loads

3.6 Drawbar pull with respect to wheel slip and lug height

The results of numerical simulation of traction performance in terms of drawbar pull for five different lug heights of 0.00776, 0.01, 0.015, 0.02, and 0.025 m and under the wheel slip ranging from 0.0 to 1.0 are presented in Fig. 10. Results show that the drawbar pull increases with lug height. For the same soil conditions and at a wheel slip of 0.2, a lug height of 0.025 m could generate a drawbar pull of 11 N, while a lug height of 0.00776 m could generate a drawbar pull of about 7.8 N. Increase in drawbar pull as lug height increases is observed to be sharp at wheel slips of 0.2 and less, after which the sharpness decreases and it tends to a more gentle increase.

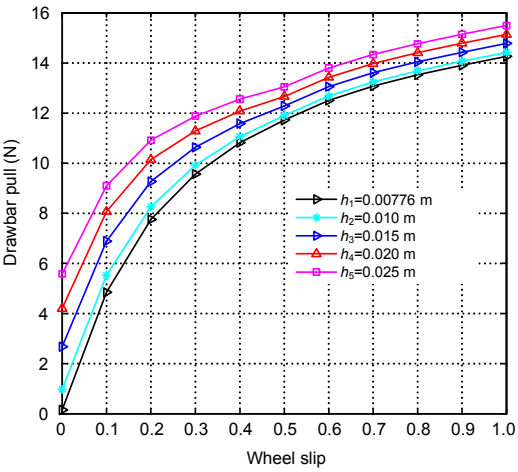

Fig. 10 Drawbar pull vs. wheel slip for different lug heights

3.7 Driving torque with respect to wheel slip and lug height

The results of numerical simulation of traction performance in terms of the driving torque for four different lug heights of 0.00776, 0.01, 0.02, and 0.03 m and under the wheel slip ranging from 0.0 to 1.0 are presented in Fig. 11. Results show that the driving torque increases with the lug height. For the same soil conditions and at a wheel slip of 0.2, a lug height of 0.03 m required a driving torque of about 3.2 N·m, while a lug height of 0.00776 m required a driving torque of about 2.1 N·m. This implies that the lug height or grouser has a significant effect on the torque.

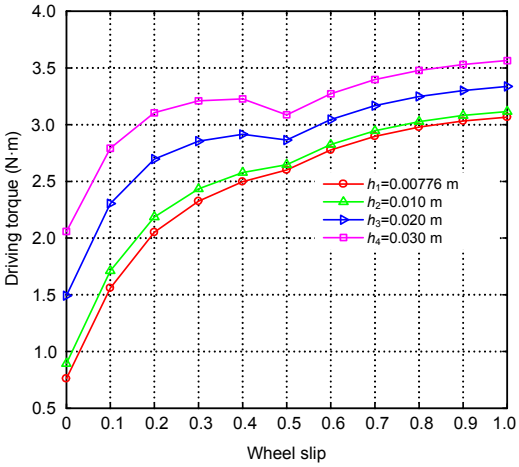

Fig. 11 Driving torque vs. wheel slip for different lug heights

4 Multiobjective optimization (MOO) problem formulation

4.1 Basic concept and application of MOO to AWMR mobility performance

An optimization problem is one requiring the determination of the optimal (maximum or minimum) value of a given function, called the objective or fitness function, subject to certain defined restrictions, or constraints placed on the variables concerned (Stroud, 2003). Optimization could also be viewed as the process of making a decision or choosing the best out of available resources to achieve the most desired results. In optimization problems, we are interested in minimizing undesirable effects and/or maximizing desirable effects. Any or both of these will form the objective of optimization from which the objective function is formulated. An optimization problem could be single objective or MOO. For MOO, the final solution of the objective functions will represent a compromise (tradeoffs) between different objectives that may be totally conflicting, partially conflicting or non-conflicting (Vanderplaats, 1984; Mastinu *et al*., 2006; Goh and Tan, 2009). A general multiobjective minimization problem can be defined as follows:

$$\begin{aligned}\min_{\boldsymbol{x}\in\boldsymbol{X}^n}\ & f_i(\boldsymbol{x})=\{f_1(\boldsymbol{x}), f_2(\boldsymbol{x}), ..., f_M(\boldsymbol{x})\}\\ \text{s.t.}\ & g(\boldsymbol{x})\geq 0,\ \ h(\boldsymbol{x})=0,\end{aligned} \tag{37}$$

where $\boldsymbol{x}$ is the vector of decision variables bounded by the decision space, $\boldsymbol{X}^{n_x}$, and f is the set of objectives to be minimized. The functions g and h are sets of inequality and equality constraints that define the feasible region of the n_x-dimensional continuous or discrete feasible solution space, respectively.

MOO problems are mostly continuous and non-linear, and the primary goal is to model the preferences of a decision maker. In this study, the objective functions to be optimized are given in Eq. (23) for drawbar pull $f_1(\boldsymbol{x})$, Eq. (36) for tractive efficiency $f_2(\boldsymbol{x})$, and Eq. (35) for dynamic traction ratio $f_3(\boldsymbol{x})$. To achieve optimum traction performance, the drawbar pull and tractive efficiency are maximized by minimizing the negative of their functions. Bekker (1969) observed that the maximum tractive force a terrain can bear increases with increasing normal force. Therefore, to avoid terrain failure and resultant slip-sinkage and immobilization of the wheel, the optimum traction performance requires the minimization of the maximum ratio of the tractive force to the normal force (Iagnemma and Dubowsky, 2004). The dynamic traction ratio DTR in Eq. (35) represents this ratio, and hence it is minimized. The objective functions depend on five parameters expressed as $\boldsymbol{x}$ in the MOO problem formulation, which include wheel radius, lug height, wheel slip, rotation angle, and wheel width. The goal of optimization in this study is to determine the set of optimized wheel design parameters for the given terrain on which the AWMR will be required to operate, the favorable ground conditions in terms of slip and sinkage, and the corresponding optimal traction parameters that will be used for mobility control. This is explained in detail in Section 5.2. To obtain the optimal set of these parameters, the MOO problem is formulated as follows:

$$\begin{aligned}\min\ & f_i(\boldsymbol{x})=\{f_1(\boldsymbol{x}), f_2(\boldsymbol{x}), f_3(\boldsymbol{x})\}\\ \text{s.t.}\ & \boldsymbol{A}\boldsymbol{x}\leq b,\ \boldsymbol{A}_{\text{eq}}\boldsymbol{x}=b_{\text{eq}},\ C(\boldsymbol{x})\leq 0,\\ & C_{\text{eq}}(\boldsymbol{x})=0,\ l_b\leq\boldsymbol{x}\leq u_b.\end{aligned} \tag{38}$$

A solution is formulated in MATLAB using GA as follows (Table 2):

$$\begin{aligned}&[\boldsymbol{x}, \boldsymbol{f}_{\text{val}}]\\ &=\text{gamultiobj}(@\text{fun}, \boldsymbol{A}, \boldsymbol{b}, \boldsymbol{A}_{\text{eq}}, \boldsymbol{b}_{\text{eq}}, \boldsymbol{l}_b, \boldsymbol{u}_b, @\text{Nlc.options...}).\end{aligned} \tag{39}$$

Herein $\boldsymbol{x}=[r, h, s, \theta, b]^{\text{T}}$ is the optimal solution that gives the optimized design parameters for the given terrain and the corresponding optimal ground interface conditions; $\boldsymbol{A}$ and $\boldsymbol{b}$ are linear inequality constraints specified by matrix $\boldsymbol{A}$ and vector $\boldsymbol{b}$, respectively; $\boldsymbol{A}_{\text{eq}}$ and $\boldsymbol{b}_{\text{eq}}$ are linear equality constraints specified by matrix $\boldsymbol{A}_{\text{eq}}$ and vector $\boldsymbol{b}_{\text{eq}}$, respectively; $\boldsymbol{l}_b$ and $\boldsymbol{u}_b$ are lower and upper bounds on the variables specified as vectors, respectively; f_{val}'s are the objective functions minimized (i.e., $f_1(\boldsymbol{x})$, $f_2(\boldsymbol{x})$, $f_3(\boldsymbol{x})$) as earlier explained; Nlc represents the non-linear constraints consisting of C and C_{eq}, which are non-linear inequalities and equalities, respectively; options are the selective parameters for optimization; fun is the anonymous function m-file containing MATLAB codes for the computation procedure with the fitness functions, and gamultiobj is the GA in the MATLAB

optimization tool box (Table 2). Generally, Eq. (39) is the command line in the MATLAB m-file that initiates and implements the MOO process with a GA as described in Section 4.2.

Table 2 Rank-based selection and niching technique: multiobjective genetic algorithm (MOGA)

No.	Description
1	Initialize variables (length of individuals, number of decision variables, generational gap, crossover rate, mutation rate, number of generations, binary representation scheme)
2	State the field
3	Initialize population
4	Begin generational loop
5	While generation is less than maximum generation
6	Assign fitness values to entire population
7	Perform visualization and fitness articulation
8	Select individuals for breeding
9	Perform cross over routines/recombine individuals
10	Apply mutation
11	Evaluate offspring/call objective function
12	Reinsert offspring into population
13	Increment counter
14	End
15	Convert chromosomes to real values

4.2 Solving the MOO problem with genetic algorithm and results

4.2.1 Introduction

Among other meta-heuristic approaches, the multiobjective evolutionary algorithm (MOEA), which is based on the Darwinian Wallace principle of 'survival-of-the-fittest', is one of the most popular stochastic search methods to solve multiobjective problems. MOEAs are preferred for optimization over the traditional algorithms based on binary methods and derivatives for some reasons; for example, in natural selection and adaptation, MOEAs have a unique advantage of being able to sample multiple solutions simultaneously. This feature provides it with a global perspective of the multiobjective problem as well as the capability to find a set of Pareto-optimal solutions in a single run. GA is one type of MOEA. It is a general adaptive algorithm that is presently widely accepted and applied in science, engineering, business, etc. due to its proven robustness as a stochastic search method. Basic components of GA include (Williams, 1995; Boyd and Vandenberghe, 2004; Marler and Arora, 2004; Konak *et al*., 2006; Miettinen, 2008; Barrico *et al.*, 2009):

1. Encoding: the algorithm encodes a set of initial optimal solutions in form of gene and chromosomes and computes their fitness in the problem region;

2. Initialization: new individuals are created by reproduction, crossover, and variation;

3. Evaluation function: new individuals are evaluated in the given environment;

4. Selection of parents: new modified parents are selected for next reproduction;

5. Genetic operators: mutation and recombination are carried out;

6. Parameter settings: this involves practice and art.

This process is repeated in a cycle (Fig. 12) for several generations and new approximate optimal solutions are chosen from the new individuals until the best fitness value is less than or equal to the value of the fitness limit specified in the options. The type of GA used in this study is the multiobjective genetic algorithm (MOGA), which uses rank-based selection and niching techniques to generate populations of non-dominated solutions of the optimization problem in a Pareto front without combining the objectives in some way (Table 2).

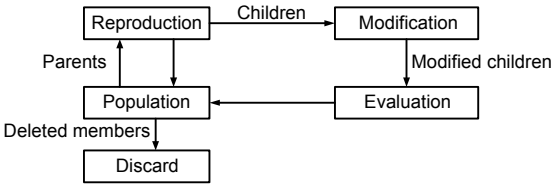

Fig. 12 Reproduction cycle for typical genetic algorithms

4.2.2 Pareto set analysis

Pareto analysis in MOO is a sort of decision theory used in GA. Two primary steps are usually involved: one is to generate the option space (population) and the other is to select the best option (non-dominated solution set). In a design where the power selection or motion control problem involves many decision variables, there are typically an infinite number of optimal solutions based on the preferences and risk assessments of the decision maker(s). Choosing from this set of solutions is usually not easy and involves tradeoffs. The final solution will be a

result of numerous tradeoffs usually aimed at making a compromise decision between attributes of conflicting variables.

In this study, five decision parameters and three objectives are considered as explained earlier. The optimization problem is based on mathematical models simulating a typical/near-real situation of AWMR mobility on rough terrain. Pareto analysis provides a decision support for determination of the optimal non-dominated solution, given a set of operating conditions or constraints (which could be linear or non-linear or both), risk profiles, and preferences. There are two primary approaches to finding the preferred or optimal solution in MOO problems. One approach, involving determining the relative importance of the variables and aggregating them into an overall objective and solving the problem, is presumed to give the optimal solution for the given set of variables. The second approach, which is adopted in this study, involves populating some optimal solutions along the Pareto frontier and selecting one based on the values of the variables for a given solution. This is actually the real essence and application of Pareto set analysis in an MOO problem. A Pareto optimal set is therefore a set of solutions that are non-dominated with respect to each other while moving from one Pareto solution to another; there is always a certain amount of sacrifice in one objective to achieve a certain amount of gain in the other.

4.2.3 Results of MOO and Pareto set analysis with GA

The results of MOO and Pareto set analysis are presented in Tables 3–8 and Figs. 13–16. Fig. 13 shows the Pareto front or set of non-dominated solutions for tractive efficiency and drawbar pull, and the numerical values are presented in Table 5. Boundary conditions showing the lower and upper bounds in this particular optimization run for the five decision variables are presented in Table 3. These boundaries have been set based on the expected design output of the designer of WMR, information available in the literature, the relevant decoupled terramechanics model and the relative specific parameters and experience of our 5-WMR. So the problem is described as a 'bound constraint' type as in Table 4. Also in Table 4, population size and Pareto fraction for the GA are set at 100 and 0.55, respectively, which are considered adequate to generate sufficient search for optimal solutions. As the MOO algorithm is run in MATLAB, after 115 generations and 11 601 function counts, the GA selected 56 best individuals considered as non-dominated solutions out of 100 individuals in the population. Average distance between individuals is 0.0051, which indicates good convergence of the MOO solution. A solution is considered to be in the vicinity of non-dominated Pareto set if it has a Euclidean distance of less than 0.05 difference from the nearest point in the Pareto set. Also in Table 4, the spread of the MOO solution is 0.1345, which shows the diversity or distribution of the generated solutions as shown on the smooth curve of the Pareto front in Fig. 13. In Fig. 13, as earlier explained, moving from one solution to another in the Pareto set usually involves tradeoffs of one objective in favour of the other. Using the horizontal (drawbar pull) axis as a reference, the Pareto front can be viewed as in three sections. Section A is between 12 and 14 N, section B is between 14 and 18 N, and section C is between 18 and 24 N.

In section A, all the solutions are in favor of objective $f_1(\boldsymbol{x})$, which is to maximize tractive efficiency. In section C, all the solutions are in favor of objective $f_2(\boldsymbol{x})$ to maximize drawbar pull. However, in section B there seems to be a good compromise in favor of the two objectives simultaneously, so the set of non-dominated solutions is selected from this section and results are presented in Table 5. For the specific soil type and condition considered, solution 5 in Table 5 is selected as the best among the set, which gives the optimized wheel design parameters as follows: wheel radius is 0.1558 m, lug height is 0.0118 m, width is 0.115 m; corresponding favorable ground conditions include: wheel slip is 0.0881 and rotation angle is 33.085°, while the optimal values for drawbar pull is 16.8715 N, tractive efficiency is 0.6142, and the dynamic traction ratio is 0.4478. Similarly, the results showing the Pareto front of non-dominated solutions for tractive efficiency and dynamic traction ratio are presented in Fig. 14 and this further buttresses the selected solution in Table 5.

In a similar way to the first MOO results discussed above, Fig. 15 shows the Pareto front or set of non-dominated solutions for tractive efficiency and drawbar pull, and the numerical values are presented in Table 8. The major difference between the first simulation and this second one is the range of slip, which is between 0.15 and 0.50 according to the relevant decoupled terramechanic model applied.

Table 3 Boundary conditions for wheel-terrain parameters for Figs. 13 and 14

Bound	Wheel radius, r (m)	Lug height, h (m)	Wheel slip, s	Rotation angle, θ (°)	Wheel width, b (m)
Lower bound (lb)	0.100	0.01	0.00	30	0.10
Upper bound (ub)	0.158	0.02	0.15	35	0.15

Table 4 Output data describing the results of MOO with GA for Figs. 13 and 14

Problem type	Number of generations	Size of population	Function count	Pareto fraction	Size of non-dominated set	Average distance	Spread
Bound-constraint	115	100	11 601	0.55	56	0.0051	0.1345

Table 5 Numerical results of Pareto set analysis with GA showing optimized wheel design parameters and corresponding ground and traction parameters for Figs. 13 and 14

Solution No.	Radius, r (m)	Lug height, h (m)	Wheel slip, s	Rotation angle, θ (°)	Width, b (m)	DP (N)	TE	DTR
1	0.1559	0.0118	0.1321	33.0277	0.1150	18.6420	0.5471	0.5002
2	0.1556	0.0119	0.0911	33.0563	0.1151	17.0295	0.6084	0.4575
3	0.1557	0.0120	0.1106	33.0334	0.1154	17.8893	0.5757	0.4818
4	0.1546	0.0193	0.1427	32.9818	0.1149	21.3672	0.5051	0.5635
5	0.1558	0.0118	0.0881	33.0850	0.1150	16.8715	0.6142	0.4478
6	0.1556	0.0124	0.0932	33.0964	0.1152	17.2964	0.6008	0.4575
7	0.1556	0.0119	0.1371	33.0391	0.1152	18.8724	0.5401	0.5054
8	0.1556	0.0118	0.1026	33.0563	0.1152	17.4991	0.5894	0.4712
9	0.1557	0.0119	0.1207	33.0391	0.1152	18.2586	0.5617	0.4870
10	0.1557	0.0120	0.1232	33.0334	0.1152	18.3791	0.5578	0.4940

Table 6 Boundary conditions for wheel-terrain parameters for Figs. 15 and 16

Bound	Wheel radius, r (m)	Lug height, h (m)	Wheel slip, s	Rotation angle, θ (°)	Wheel width, b (m)
Lower bound (lb)	0.100	0.01	0.15	30	0.10
Upper bound (ub)	0.158	0.02	0.50	35	0.15

Table 7 Output data describing the results of MOO with GA for Figs. 15 and 16

Problem type	Number of generations	Size of population	Function count	Pareto fraction	Size of non-dominated set	Average distance	Spread
Bound-constraint	128	100	12 901	0.55	56	0.0021	0.1324

Table 8 Numerical results of Pareto set analysis with GA showing optimized wheel design parameters and corresponding ground and traction parameters for Figs. 15 and 16

Solution No.	Radius, r (m)	Lug height, h (m)	Wheel slip, s	Rotation angle, θ (°)	Width, b (m)	DP (N)	TE	DTR
1	0.1564	0.0122	0.1542	33.0277	0.1420	25.4273	0.5661	0.4634
2	0.1563	0.0123	0.2437	32.8443	0.1454	26.6283	0.4903	0.5465
3	0.1563	0.0125	0.1881	32.8615	0.1455	25.9915	0.5353	0.4891
4	0.1563	0.0123	0.2224	32.8672	0.1442	26.4042	0.5071	0.5221
5	0.1563	0.0122	0.1640	32.9933	0.1456	25.5673	0.5574	0.4779
6	0.1563	0.0122	0.2523	32.8171	0.1459	26.7052	0.4838	0.5681
7	0.1564	0.0123	0.2476	32.6438	0.1455	26.6658	0.4873	0.5542
8	0.1564	0.0122	0.2585	32.9990	0.1461	26.7561	0.4790	0.5830
9	0.1563	0.0122	0.1840	32.7927	0.1457	25.8739	0.5396	0.4826
10	0.1563	0.0122	0.1872	32.6724	0.1460	25.9240	0.5368	0.4925

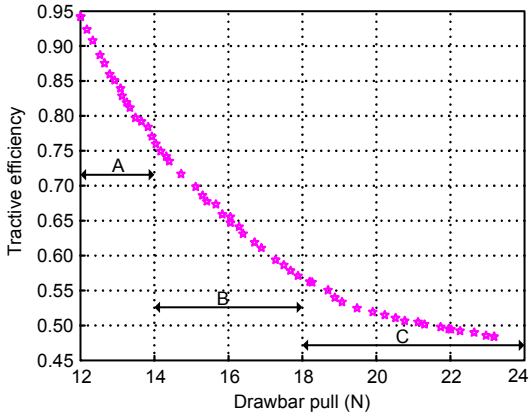

Fig. 13 Pareto front of non-dominated solutions for tractive efficiency vs. drawbar pull after 115 generations at W=36.75 N and 0.0<s<0.15

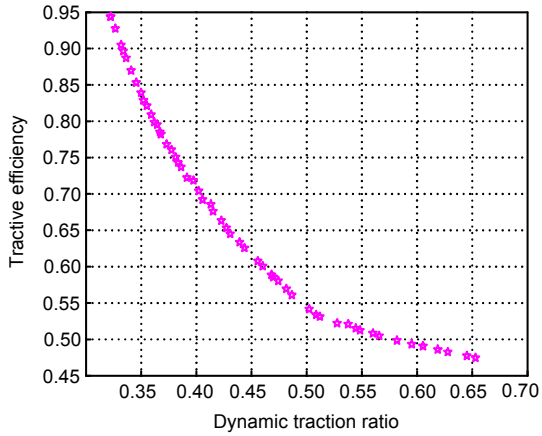

Fig. 14 Pareto front of non-dominated solutions for tractive efficiency vs. the dynamic traction ratio after 115 generations at W=36.75 N and 0.0<s<0.15

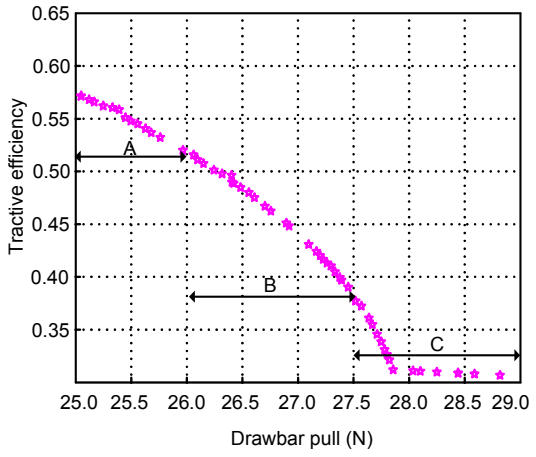

Fig. 15 Pareto front of non-dominated solutions for tractive efficiency vs. drawbar pull after 128 generations at W=36.75 N and 0.15<s<0.50

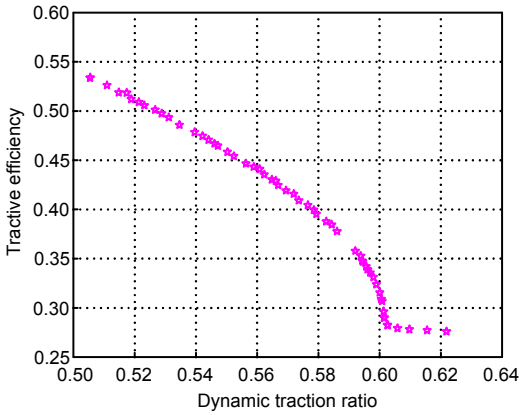

Fig. 16 Pareto front of non-dominated solutions for tractive efficiency vs. the dynamic traction ratio after 128 generations at W=36.75 N and 0.15<s<0.50

Based on experimental results of Ding *et al*. (2011a), this model had divided slip ratios into three phases:

1. Rising phase (0.0–0.2), during which the drawbar pull and driving torque increase rapidly and tractive efficiency attains the maximum value. This happens when the WMR is moving on a relatively flat terrain.

2. Transitional phase (0.2–0.6), during which the drawbar pull and driving torque increase slowly and tractive efficiency decreases rapidly. This phase occurs mainly when the WMR is climbing up a slope with a large rotation angle or negotiating an obstacle.

3. High-sinkage phase (0.6–1.0), during which slip-sinkage is the most severe compared to the first two stages. This stage should generally be identified and noted in developing a control algorithm and be avoided as this can lead to total immobilization of the wheels and a subsequent motion failure. Boundary conditions showing the lower and upper bounds in this particular optimization run for the five decision variables are presented in Table 6.

Also in Table 7, population size and Pareto fraction for the GA are set at 100 and 0.55, respectively, which are considered adequate to generate sufficient search for optimal solutions. As the MOO algorithm is run in MATLAB, after 128 generations and 12901 function counts the GA selected 56 best individuals considered as non-dominated solutions out of 100 individuals in the population. Average distance between individuals is 0.0021, while the spread is 0.1324 as presented in Table 7, which indicate good convergence and diversity of the MOO solution, respectively.

In Fig. 15 and using the horizontal (drawbar pull) axis as reference, the Pareto front is divided into three sections as follows: section A is between 25 and 26 N, section B is between 26 and 27.5 N, and section C is between 27.5 and 29 N. In a similar analysis to the first simulation, No. 4 solution in Table 8 is selected as the best non-dominated solution among the Pareto set for the MOO as follows: wheel radius is 0.1563 m, lug height is 0.0123 m, width is 0.14442 m, wheel slip is 0.2224, rotation angle is 32.8672°, drawbar pull is 26.4042 N, tractive efficiency is 0.5071, and the dynamic traction ratio is 0.5221.

Results showing the Pareto front of non-dominated solutions for tractive efficiency and dynamic traction ratio are presented in Fig. 16 and this further buttresses the selected solution in Table 8.

5 Experimental verification, discussion, and application of results

5.1 Experimental verification

The numerical results of MOO and Pareto set analysis with GA as presented in Tables 5 and 8 give the non-dominated solutions of the MOO problem of traction performance. The optimized values of design parameters such as wheel radius, width, and lug height with respect to relevant key traction parameters are obtained as presented.

From Table 5, MOO results of Nos. 1–5 and 10 are plotted and compared with experimental data and results from Ding *et al*. (2011a) (Fig. 17). In the experiments as presented in Ding *et al*. (2011a), the optimal tractive efficiency TE for wheel 32 of radius of 157.35 mm, width of 165 mm, and a lug height of 10 mm is about 0.54, and this occurred at a slip ratio of roughly 0.15. The GA for MOO had selected the optimized wheel radius from a range between 100 and 158 mm; similarly, the ranges of values for width and lug height are as shown in Table 5. Fitting the non-dominated solution data from Table 5, Nos. 1–5 and 10 (MOO_1 to MOO_5 and MOO_10) into the decoupled closed form traction performance model for tractive efficiency and slip ratio gives the graphical results as presented in Fig. 17.

As it can be seen, the tractive efficiencies from MOO are all between 0.54 and 0.60 occurring around wheel slips of 0.15 and 0.20. This shows that there is a good agreement between the MOO and experimental results, and hence the results can be accepted as valid.

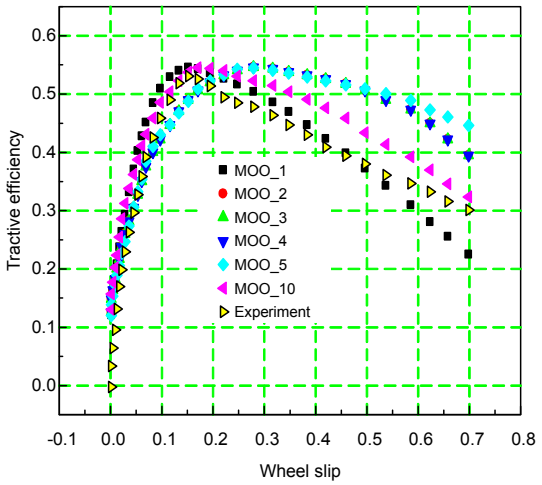

Fig. 17 Experimental validation of non-dominated solutions of MOO using GA for tractive efficiency with respect to wheel slip

5.2 Application of MOO results to AWMR traction control

In applying MOO theory towards the optimal mobility performance of AWMR in rough terrain, there are two stages (Fig. 18): offline and online operations. In the offline stage, the MOO algorithm is applied in design to determine the optimum vehicle parameters that give the best traction performance for a given terrain, such as the total mass that determines vertical load W, wheel radius r, width b, and lug height h. This consideration is based on the fact that for terrestrial missions, the task and hence the environment where the WMR will operate is usually a predefined entity, for instance, mining, agriculture, search, and rescue. Similarly, planetary rovers could be designed for mission on the Moon or Mars. Therefore, researchers and organizations involved in such explorations have carried out some basic research to know the specific soil characteristics of the various terrains over which the WMR will be required to move. So, the terrain properties can be known and used as input parameters in the MOO algorithm to determine optimum vehicle parameters for each particular terrain in question. It should be pointed out that such terrain parameters used as inputs in offline operations may actually have some slight variations in

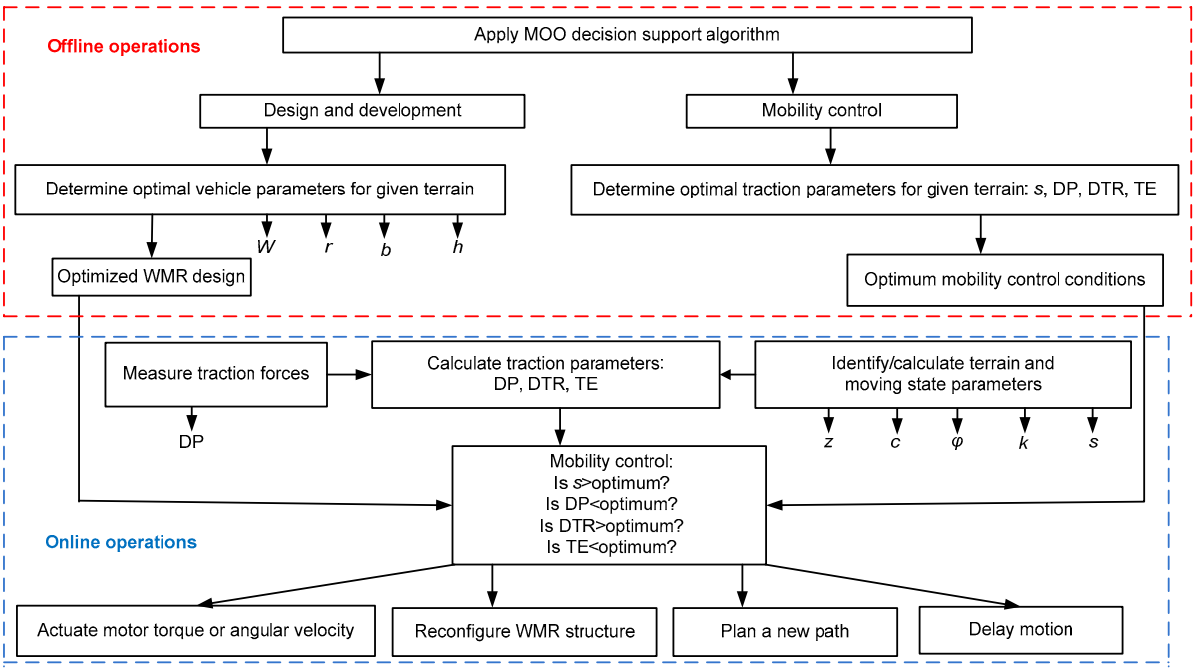

Fig. 18 Block diagram of the algorithm for applying MOO to motion control of AWM

actual real time situations of WMR mobility on rough terrain. However, the slight variations are assumed negligible and also certain tolerance can be given. Similarly, for the given terrain and using the traction models, the optimal traction parameters such as slip, drawbar pull, tractive efficiency, and dynamic traction ratio can be determined with the MOO algorithm based on design parameters. The second stage is online and has to do with mobility control when the WMR is actually moving over the rough terrain. Essentially, there is no real-time optimization, and we use only the result of stage one as the condition for control. This stage consists of several aspects: (1) Identify/calculate terrain properties and moving state variables such as cohesion, internal friction angle, shear deformation modulus, slip, and sinkage. Many researchers have studied and more are presently researching methods for online terrain parameter identification for WMR in rough terrain. (2) Measure the force at the wheel-terrain contact using a Force/Torque sensor, that is the drawbar pull. (3) Calculate traction parameters such as tractive efficiency and the dynamic traction ratio. (4) Apply the control decisions (Is wheel slip greater than the prescribed optimum value? Is drawbar pull less than optimum? Is tractive efficiency less than optimum? Is dynamic traction ratio greater than optimum? etc.). (5) Actuate the controller (e.g., vary motor torque or angular velocity; reconfigure robot structure; plan a new path or delay motion) (Fig. 18). At this point the actions of the controller through the control software via an onboard personal computer helps to maintain the wheel-terrain contact conditions at the desired optimum, and hence optimum mobility is realized.

According to Ding *et al*. (2011a), PE=DP·r_s/T, denoting the drawbar pull efficiency, which is the efficiency with which the tractive force is transformed into the effective drawbar pull, PC=F_{DP}·F_N=DP/W, denoting the drawbar pull coefficient that is the drawbar pull caused by a unit normal force, and TC=T/(F_N·r_s), denoting the tractive coefficient which implies the tractive force caused by the torque T of the motor and reduction gears of the rover for a unit normal load on the wheel. From the foregoing analysis, we have the following expression for PE:

$$\mathrm{PE}=\frac{\mathrm{PC}}{\mathrm{TC}}=\frac{\mathrm{DP}}{W}\Big/\left(\frac{T}{W}\cdot r_s\right). \tag{40}$$

Also recalling as earlier stated that tractive efficiency is given as TE=[DP·r_s(1−s)]/T, it is obvious that modulating angular velocity and torque of the motor through the procedure suggested in Fig. 18 will provide effective traction and motion control of an

AWMR in rough terrain. The drawbar pull coefficient (PC) can be used to evaluate the pulling ability of a wheel under different vertical loads as well as the trafficability, such as the slope-climbing ability of the rover over rough terrain. The MOO algorithm developed could be adapted for optimal WMR designs and determination of optimal control conditions for any other terrain of interest. For instance, a designer will know from this kind of analysis that choosing a particular wheel radius, width, and lug height would help to achieve a certain level of drawbar pull and traction efficiency, given the terrain characteristics. This work can also be applied for power selection, that is, selecting a motor for the WMR to provide the required torque.

6 Conclusions and future work

This paper presents a numerical analysis and MOO of traction performance based on decoupled closed form terramechanics, which have considered key soil, vehicle and interface parameters in modeling and predicting traction and mobility performance of AWMR in rough terrain. The following conclusions are made from the study:

1. Application of terramechanics to the study of AWMR mobility is generally a new area of research currently receiving attention globally. This paper proposes a method for the application of closed form terramechanics, which has considered more wheel-terrain variables than the integral open form models together with MOO for achieving optimized design, mobility performance, and control of AWMR in rough terrain.

2. WMR parameters, such as wheel radius, width, lug height, and normal load, are important design parameters having significant impact on traction performance of AWMR in rough terrain.

3. Tractive efficiency with respect to wheel slip increases as wheel radius and lug height increase, until a certain maximum value that occurs around a wheel slip of 0.2, after which it decreases sharply. Also, drawbar pull and driving torque with respect to wheel slip increase proportionally with normal load.

4. For any given terrain, the WMR design parameters can be optimized to achieve an optimum traction and hence mobility performance using the MOO method with a genetic algorithm (GA) in MATLAB. For the specific soil condition considered in this study, MOO results give the optimized wheel design parameters such as radius, lug height, width, and normal load, and the corresponding favourable traction parameters, such as wheel slip, rotation angle, tractive efficiency, drawbar pull, and dynamic traction ratio, which can all be applied for mobility control.

5. In the MOO problem formulated, the GA known for its robustness in handling MOO problems selects a set of non-dominated solutions called the Pareto set by populating them graphically on the Pareto front. This enables the decision maker who wants to optimize the design of WMR to choose the best according to his/her specific problem and also be able to make optimized decisions in his/her mobility control algorithm, of which an overview has been discussed in this paper.

6. Comparison of MOO results with experimental results showed good agreement, hence confirming the validity of this approach to optimize the design and mobility performance of AWMR in rough terrain.

Future work will focus on sensor fusion approach (fifth wheel, inertial measurement unit, and vision camera) to wheel slippage detection, estimation, and compensation, and online terrain parameter identification for motion control of AWMRs in rough terrain.

Acknowledgements

The authors are grateful to Dr. Liang DING of Harbin Institute of Technology, China for making some of his relevant published papers available and for being available for useful discussions with them.

References

Barrico, C., Antunes, C.H., Pire, D.F., 2009. Robustness analysis in evolutionary multi-objective optimization applied to VAR planning in electrical distribution networks. *LNCS*, **5482**:216-227. [doi:10.1007/978-3-642-01009-5_19]

Bekker, M.G., 1956. Theory of Land Locomotion. University of Michigan Press, Ann Arbor, MI.

Bekker, M.G., 1960. Off-the-Road Locomotion. University of Michigan Press, Ann Arbor, MI.

Bekker, M.G., 1969. Introduction to Terrain-Vehicle Systems.

University of Michigan Press, Ann Arbor, MI.

Boyd, S., Vandenberghe, L., 2004. Convex Optimization. Cambridge University Press, UK.

Ding, L., Yoshida, K., Nagatani, K., Gao, H., Deng, Z., 2009. Parameter Identification for Planetary Soil Based on a Decoupled Analytical Wheel-Soil Interaction Terramechanics Model. Int. Conf. on Intelligent Robots and Systems, p.4122-4127. [doi:10.1109/IROS.2009.5354538]

Ding, L., Gao, H., Deng, Z., Nagatani, K., Yoshida, K., 2011a. Experimental study and analysis on driving wheel's performance for planetary exploration rovers moving in deformable soil. *J. Terramech.*, **48**(1):27-45. [doi:10.1016/j.jterra.2010.08.001]

Ding, L., Deng, Z., Gao, H., 2011b. Planetary rover's wheel-soil interaction mechanics: new challenges and applications for wheeled mobile robots. *Intell. Serv. Rob.*, **4**(1):17-38. [doi:10.1007/s11370-010-0080-5]

Freitas, G., Gleizer, G., Lizarralde, F., Hsu, L., Dos Reis, N.R.S., 2010. Kinematic reconfigurability control for an environmental mobile robot operating in the Amazon rain forest. *J. Field Rob.*, **27**(2):197-216. [doi:10.1002/rob.20334]

Goering, C.E., 1989. Engine and Tractor Power. American Society of Agricultural Engineers, USA.

Goh, C.K., Tan, K.C., 2009. Evolutionary Multi-objective Optimization in Uncertain Environments. Springer Verlag, Berlin Heidelberg.

Gustafsson, F., 1997. Slip-based tire-road friction estimation. *Automatica*, **33**(6):1087-1099. [doi:10.1016/S0005-1098(97)00003-4]

Iagnemma, K., Dubowsky, S., 2004. Traction control of wheeled robotic vehicles in rough terrain with application to planetary rovers. *Int. J. Rob. Res.*, **23**(10-11):1029-1040. [doi:10.1177/0278364904047392]

Iagnemma, K., Ward, C.C., 2009. Classification-based wheel slip detection and detector fusion for mobile robots on outdoor terrain. *Auton. Rob.*, **26**(1):33-46. [doi:10.1007/s10514-008-9105-8]

Iagnemma, K., Shibly, H., Rzepniewski, A., Dubowsky, S., 2001. Planning and Control Algorithms for Enhanced Rough-Terrain Rover Mobility. Proc. 6th Int. Symp. on Artificial Intelligence, Robotics and Automation in Space, i-SAIRAS.

Iagnemma, K., Golda, D., Spenko, M., Dubowsky, S., 2002. Experimental Study of High-Speed Rough-Terrain Mobile Robot Models for Reactive Behaviours. Experimental Robotics VIII, p.654-663. [doi:10.1007/3-540-36268-1_60]

Janosi, Z., Hanamoto, B., 1961. Analytical Determination of Drawbar Pull as a Function of Slip for Tracked Vehicles in Deformable Soils. Proc. 1st Int. Conf. on Terrain-Vehicle Systems, p.707-726.

Konak, A., Coit, D.W., Smith, A.E., 2006. Multi-objective optimization using genetic algorithms: a tutorial. *Rel. Eng. Syst. Safety*, **91**(9):992-1007. [doi:10.1016/j.ress.2005.11.018]

Konjicija, S., Avdagić, Z., 2009. Evolutionary Multi-objective Approach to Control of Mobile Robot in Unknown Environment. 22nd Int. Symp. on Information, Communication and Automation Technologies, p.1-8. [doi:10.1109/ICAT.2009.5348429]

Lindgren, D.R., Hague, T., Smith, P.J.P., Marchant, J.A., 2002. Relating torque and slip in an odometric model for an autonomous agricultural vehicle. *Auton. Rob.*, **13**(1):73-86. [doi:10.1023/A:1015682206018]

Liu, W., Winfield, A.F.T., 2010. Modeling and optimization of adaptive foraging in swarm robotic systems. *Int. J. Rob. Res.*, **29**(14):1743-1760. [doi:10.1177/0278364910375139]

Marler, R.T., Arora, J.S., 2004. Survey of multi-objective optimization methods for engineering. *Struct. Multidisc. Optim.*, **26**(6):369-395. [doi:10.1007/s00158-003-0368-6]

Mastinu, G., Gobbi, M., Miano, C., 2006. Optimal Design of Complex Mechanical Systems: with Application to Vehicle Engineering. Springer-Verlag, Berlin Heidelberg.

Miettinen, K., 2008. Introduction to Multiobjective Optimization: Noniterative Approaches. Springer-Verlag, Berlin Heidelberg.

Ojeda, L., Borenstein, J., 2004. Methods for the reduction of odometry errors in over-constrained mobile robots. *Auton. Rob.*, **16**(3):273-286. [doi:10.1023/B:AURO.0000025791.45313.01]

Reina, G., 2006. Methods for Wheel Slip and Sinkage Estimation in Mobile Robots. *In*: Yussof, H. (Ed.), Robot Localization and Map Building. InTech, p.561-578.

Sato, M., Ishii, K., 2010. Simultaneous optimization of robot structure and control system using evolutionary algorithm. *J. Bion. Eng.*, **7**:S185-S190. [doi:10.1016/S1672-6529(09)60234-1]

Schenker, P., Huntsberger, T., Pirjanian, P., Dubowsky, S., Iagnemma, K., Sujan, V., 2003. Rovers for Intelligent, Agile Traverse of Challenging Terrain. 11th Int. Conf. on Advanced Robotics.

Schreiber, M., Kutzbach, H.D., 2008. Influence of soil and tire parameters on traction. *Res. Agr. Eng.*, **54**(2):43-49.

Shibly, H., Iagnemma, K., Dubowsky, S., 2005. An equivalent soil mechanics formulation for rigid wheels in deformable terrain, with application to planetary exploration rovers. *J. Terramech.*, **42**(1):1-13. [doi:10.1016/j.jterra.2004.05.002]

Sohne, W., 1958. Fundamentals of pressure distribution and soil compaction under tractor tires. *Agr. Eng.*, **39**(5):290.

Stroud, K.A., 2003. Advanced Engineering Mathematics. Palgrave MacMillan, Houndmills.

Vanderplaats, G.N., 1984. Numerical Optimization Techniques for Engineering Design with Applications. McGraw-Hill, New York.

Williams, W., 1995. Genetic Algorithms: a Tutorial. Available from http://www.dbai.tuwien.ac.at/staff/musliu/.../Class9GATutorial.ppt [Accessed on Aug. 2, 2012].

Wong, J.Y., 2001. Theory of Ground Vehicles. John Willey and Sons, New York, p.91-128.

Wong, J.Y., 2010. Terramechanics and Off-Road Vehicle Engineering. Elsevier, p.1-10.

Wong, J.Y., Reece, A.R., 1967a. Prediction of rigid wheel performance based on the analysis of soil-wheel stresses part I. Performance of driven rigid wheels. *J. Terramech.*, **4**(1):81-98. [doi:10.1016/0022-4898(67)90105-X]

Wong, J.Y., Reece, A.R., 1967b. Prediction of rigid wheel performance based on the analysis of soil-wheel stresses part II. Performance of towed rigid wheels. *J. Terramech.*, **4**(2):7-25. [doi:10.1016/0022-4898(67)90047-X]

Xu, H., Zhang, Z.Y., Khalil, A., Kai, X., Gao, X.Z., 2011. Prototypes selection by multi-objective optimal design: application to a reconfigurable robot in sandy terrain. *Ind. Rob.*, **38**(6):599-613. [doi:10.1108/01439911111179110]

Yoshida, K., 2003. Slip, Traction Control, and Navigation of a Lunar Rover. 7th Int. Symp. on Artificial Intelligence, Robotics and Automation in Space.

Yoshida, K., Hamano, H., 2002. Motion dynamics and control of a planetary rover with slip-based traction model. *Proc. SPIE*, **4715**:275-286. [doi:10.1117/12.474459]

Young, R.N., Fattah, E.A., Kiadas, N., 1984. Development in Agricultural Engineering. Vehicle Traction Mechanics. Elsevier, Amsterdam, p.45-94.

Zoz, F.M., Grisso, R.D., 2003. Traction and Tractor Performance. ASAE Distinguished Lecture Series, Tractor Design, p.1-45.